UNIFYING LATENT TENSORIZED GRAPH LEARNING AND REPRESENTATION-INDUCED VIEW RECOVERY FOR INCOMPLETE MULTI-VIEW CLUSTERING

Anonymous authors
Paper under double-blind review

ABSTRACT

Incomplete multi-view clustering (IMVC) aims to address the challenge of discovering consistent information across heterogeneous multi-view data with missing views, a scenario frequently encountered in real-world applications. Although several remarkable and representative methods have been proposed to recover the missing information, they often suffer from either suboptimal graph construction or inaccurate view recovery, constrained by the lack of well-connected representations that can simultaneously support consistent structural learning and accurate view completion. In this paper, we propose a novel framework, **TGRS** (Tensorized Graph learning with Representation-induced Smooth recovery), which unifies latent tensorized graph learning and representation-induced view recovery in a joint optimization scheme. Specifically, the tensorized graph learning captures high-order cross-view structural correlations, while the smooth representation learning guides accurate recovery of missing views through low-rank and manifold-preserving constraints. This synergy enables robust representation learning. We derive efficient closed-form solutions for each subproblem, ensuring monotonic convergence. Extensive experiments on eight real-world multi-view datasets demonstrate that TGRS-IMVC consistently outperforms state-of-the-art IMVC methods across a range of missing ratios. Ablation studies and parameter sensitivity analyses further validate the effectiveness and stability of the proposed components. paragraph.

1 INTRODUCTION

The multi-view clustering (MVC) paradigm aims to leverage both consistent and complementary information across heterogeneous data modalities—such as visual, textual, and sensor-based inputs—in order to enhance clustering performance Chao et al. (2021); Chen et al. (2020); Li et al. (2019); Zhang et al. (2017). However, most conventional MVC methods are developed under the ideal assumption that data is fully available across all views. In practice, this assumption is often violated, as real-world applications frequently involve incomplete multi-view data, where the same samples may be missing in one or more views. This results in incompatibility among views and poses significant challenges in discovering both consistency and complementary informationChao et al. (2022); Li et al. (2014); Wen et al. (2023a).

The prevalence of incomplete data has motivated the development of incomplete multi-view clustering (IMVC) methods, which aim to maintain robust clustering performance even when certain views are partially missing or entirely absent. To this end, a variety of IMVC approaches have been proposed to mitigate the adverse effects of missing views and to improve clustering robustness by exploiting both consistency and complementarity through different strategies. Among these, matrix completion-based methods exploit the inherent low-rank structure of multi-view data to impute missing entries while preserving cross-view correlations Shao et al. (2015); Rai et al. (2016). For instance, DAIMC employs a weighted semi-nonnegative matrix factorization framework that incorporates instance alignment constraints to construct a shared latent feature matrix, while a consensus basis matrix further alleviates the impact of missing entries Hu & Chen (2018). Graph-based methods tackle data incompleteness by adaptively learning neighborhood structures Cui et al. (2022); Guo & Ye (2019). For example, Liu et al. proposed a partial graph propagation approach that infers missing graph entries corresponding to absent data Liu et al. (2023a). Kernel-based nonlinear embedding methods

Reviewers: please read the Reviewer Guidelines (iclr.cc/Conferences/2027/ReviewerGuidelines) and the AI Policy for Reviewers (iclr.cc/Conferences/2027/AIPolicyForReviewers). If you used AI to expand, edit, or polish your review, please provide the input text to the LLM. Better still, consider skipping the LLM and submitting your original text: we, and the authors, are much more interested in your unedited thoughts than in what an LLM has to say. AI-assisted or not, you are putting your name and reputation behind your review: LLM-generated falsehoods, hallucinations or misrepresentations are subject to disciplinary action, which may include desk-rejecting all papers you have authored.

provide further advantages in IMVC tasks by preserving complex data geometries Liu et al. (2021b); Zhang et al. (2021). For example, Liu et al. proposed a kernel completion algorithm that jointly learns a consensus clustering matrix, imputes each incomplete kernel matrix, and simultaneously optimizes the corresponding permutation matrices Liu et al. (2018). In addition, missing-view recovery methods seek to reconstruct absent modalities by inferring shared information from available views Liu et al. (2021a); Lin et al. (2021). For example, some approaches leverage generative adversarial networks (GANs) to generate missing data Xu et al. (2019), thereby improving cross-view alignment and enhancing downstream clustering performance.

Although these methods have demonstrated promising results, several challenges remain unresolved. Most existing IMVC approaches either struggle to effectively capture structural information across all views or produce inaccurate view recovery. These limitations largely stem from the absence of well-connected representations that can simultaneously facilitate consistent structural learning and reliable view completion, ultimately leading to suboptimal clustering performance.

To address these issues, we propose a novel framework, termed **TGRS** (Tensorized Graph learning with Representation-induced Smooth recovery), which unifies latent tensorized graph learning and representation-induced view recovery within a joint optimization scheme. Specifically, to enable accurate imputation of missing data, we introduce a smooth representation learning module that guides reliable recovery of incomplete views. Moreover, this smooth representation is jointly optimized with graph learning, thereby facilitating the discovery of well-defined cluster structures. In parallel, the tensorized graph learning module captures high-order cross-view structural correlations by leveraging the learned representations. Overall, tensorized graph learning enhances the robustness of representation learning, while representation learning alleviates the challenges of missing data and simultaneously strengthens graph construction. Through this unified framework, graph learning, representation learning, and view recovery reinforce one another in a mutually beneficial manner, ultimately improving clustering performance under incomplete multi-view settings. The main contributions of this work can be summarized as follows:

- We propose a novel framework that jointly integrates smooth representation learning, tensorized graph learning, and missing view recovery within a single optimization scheme.
- We design a smooth self-representation mechanism that encodes shared latent structures across observed and missing data. This enables accurate recovery of missing views while simultaneously producing discriminative representations for clustering.
- We conduct comprehensive experiments on eight real-world multi-view datasets under different missing ratios. Results demonstrate that our method consistently outperforms seven state-of-the-art IMVC baselines.

2 Related Work

The Incomplete multi-view clustering (IMVC) has attracted increasing attention in recent years because of its ability to handle missing views while preserving cross-view consistency. Existing methodsLi et al. (2022); Liu et al. (2022); Tang & Liu (2022); Wen et al. (2023c); Xu et al. (2022) can be broadly categorized into three groups: matrix factorization-based methods, graph-based methods, and missing-view recovery methods.

A representative category of IMVC methods is based on matrix factorization, which leverages low-rank decompositions to uncover latent shared and view-specific structures across multiple incomplete views Hu & Chen (2019); Rai et al. (2016); Zhao et al. (2021). For example, Shao et al. proposed MIC (Multiple Incomplete Views Clustering) Shao et al. (2015), which employs low-rank matrix completion to impute missing features. To better preserve geometric coherence during imputation, Liu et al. proposed IMC-NLT, a unified framework that integrates non-negative matrix factorization for dimensionality reduction and missing-view pre-filling with low-rank tensor fusion to capture high-order correlations across views, followed by consensus representation learning to ensure multi-view alignment Liu et al. (2023c).

In addition, graph-based IMVC methods aim to exploit both consistent and complementary information by dynamically learning affinity structures while simultaneously inferring the relationships among missing samples Cui et al. (2022); Guo & Ye (2019); Liu et al. (2023b); Wen et al. (2020). For example, Liang et al proposed a graph-based incomplete multi-view clustering framework that

jointly learns low-rank data reconstruction, view-specific projections, and a unified graph through consistency-guided optimization to handle missing views and exploit cross-view correlationsLiang et al. (2024). Additionally, Zhang et al. developed a two-step graph propagation framework for incomplete multi-view clustering that first completes a self-guided global graph, then propagates view-specific partial graphs under its guidance, and captures high-order correlations via low-rank tensor learning to achieve robust clustering with missing views Zhang et al. (2024).

3 METHOD

3.1 THE PROPOSED MODEL

Notations and Problem Setting. In this study, we adopt the following notation conventions: matrices are denoted by bold uppercase letters (e.g., $\mathbf{M}$), vectors by bold lowercase letters (e.g., $\mathbf{m}$), and scalars by italic letters (e.g., m). For a matrix $\mathbf{M}$, its i-th row is $\mathbf{m}_i$, the ij-th element is m_{ij}, its transpose by $\mathbf{M}^\top$, its trace by $\mathrm{tr}(\mathbf{M})$, Frobenius norm is $\|\mathbf{M}\|_F$, and vector 2-norm is $\|\mathbf{m}\|$. We assume a dataset comprising n samples $\{\mathbf{x}_i\}_{i=1}^n$, each with V views. Each sample $\mathbf{x}_i$ is represented as a concatenation of view-specific feature vectors:

$$\mathbf{x}_i = \left[\mathbf{x}_i^{(1)}, \ldots, \mathbf{x}_n^{(V)}\right] \in \mathbb{R}^{1\times d} \tag{1}$$

where $\mathbf{x}_i^{(v)} \in \mathbb{R}^{1\times d^{(v)}}$ and $d = \sum_{v=1}^V d^{(v)}$. For incomplete multi-view data, we use the symbols $\mathbf{o}$ and $\mathbf{m}$ to denote the index sets of observed and missing entries, respectively, in each view. For the v-th view, the feature vector $\mathbf{X}^{(v)}$ of a given sample can be partitioned as:

$$\mathbf{X}^{(v)} = \left[\mathbf{X}_{\mathbf{o}}^{(v)}, \mathbf{X}_{\mathbf{m}}^{(v)}\right] \tag{2}$$

where $\mathbf{X}_{\mathbf{o}}^{(v)}$ and $\mathbf{X}_{\mathbf{m}}^{(v)}$ correspond to the observed and missing parts of the data, respectively. In this work, we aim to simultaneously perform representation learning, data recovery, and consistent structural learning within a unified optimization framework. Specifically, the proposed model is formulated as:

$$\begin{aligned}&\min_{\mathbf{Z}^{(v)},\mathbf{G}^{(v)},\mathbf{X}_{\mathbf{m}}^{(v)}} \sum_{v=1}^V \left\{\Phi\left(\mathbf{Z}^{(v)}, \left[\mathbf{X}_{\mathbf{o}}^{(v)}, \mathbf{X}_{\mathbf{m}}^{(v)}\right]\right) + \Psi\left(\mathbf{Z}^{(v)}, \mathbf{G}^{(v)}\right)\right\} \\ &+ \sum_{v=1}^V \mathcal{R}(\mathbf{G}^{(v)}).\end{aligned} \tag{3}$$

where $\Phi(\cdot)$ denotes the reconstruction term that recovers missing data while learning the latent representation $\mathbf{Z}^{(v)}$, $\Psi(\cdot)$ encodes the consistency constraint between the learned representation and the view-specific graph $\mathbf{G}^{(v)}$, and $\mathcal{R}(\cdot)$ is a regularization term on the graph structure.

Tensorized Graph Learning. Since certain views contain missing data and the original observations are corrupted by noise, as shown in Eq. (3) **??**, our goal is to learn a structural graph $\mathbf{S}^{(v)}$ from the learned representations via $\Phi\left(\mathbf{Z}^{(v)}, \left[\mathbf{X}_{\mathbf{o}}^{(v)}, \mathbf{X}_{\mathbf{m}}^{(v)}\right]\right)$, which integrates both observed and recovered features. Moreover, to capture consistent structural patterns across views, we introduce a tensorized graph learning framework that jointly models all view-specific affinity matrices $\mathbf{S}^{(v)}$ within a unified tensor representation. This is coupled with a high-order regularization term $\mathcal{R}$, applied to the tensor, to promote cross-view consistency based on the learned representations. Specifically, we optimize:

$$\begin{aligned}&\min_{\mathbf{G}^{(v)}} \sum_{v=1}^V \Phi\left(\mathbf{Z}^{(v)}, \left[\mathbf{X}_{\mathbf{o}}^{(v)}, \mathbf{X}_{\mathbf{m}}^{(v)}\right]\right) \\ &+ \sum_{v=1}^V \sum_{v=1}^V \left\|\mathbf{Z}_i^{(v)} - \mathbf{Z}_j^{(v)}\right\|_2^2 \mathbf{S}_{i,j}^{(v)} + \alpha \left\|\mathbf{S}^{(v)}\right\|_F^2 + \gamma \left\|\mathcal{S}\right\|_{\circledast} \\ &s.t.\ \ {\mathbf{S}_i^{(v)}}^\top \mathbf{1} = 1; \mathbf{S}^{(v)} \succeq 0.\end{aligned} \tag{4}$$

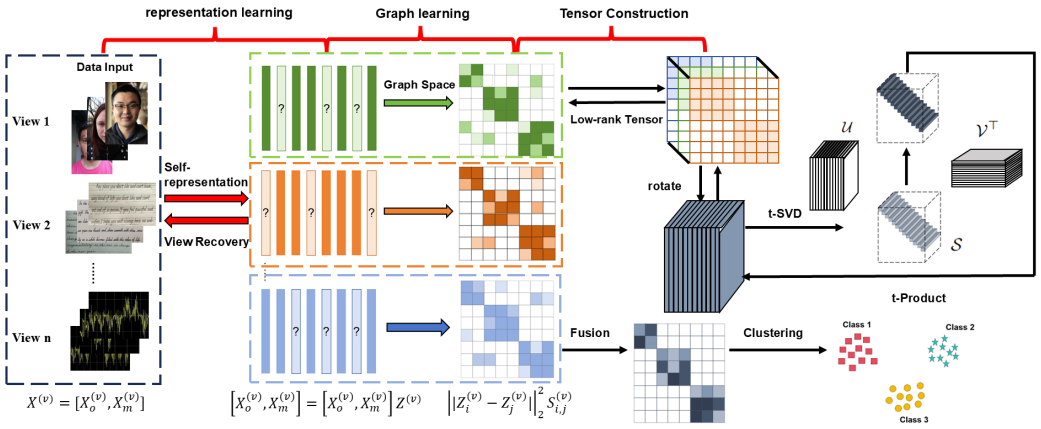

Figure 1: Overview of the proposed method. The framework jointly integrates smooth representation learning, representation-induced view recovery, and tensorized graph learning within a unified optimization scheme. Smooth representations guide accurate recovery of missing views, which in turn enhance graph construction. Tensorized graph learning captures high-order structural consistency across views, and the final consensus graph is used for spectral clustering.

where $\mathbf{Z}_i^{(v)}$ denotes the representation of the i-th sample in the v-th view, and $\mathbf{S}^{(v)} \in \mathbb{R}^{n\times n}$ is the affinity graph for the v-th view. The tensor $\mathcal{S}$ is formed by stacking all affinity graphs $\mathbf{S}^{(v)}{}_{v=1}^{V}$ along a new dimension, and $|\mathcal{S}|_{\circledast}$ denotes a tensor regularization term that enforces global consistency among views. Parameters α and γ control the regularization strengths.

Representation Induced View Recovery. For each view, we aim to learn representations from the available data such that these representations capture common view-specific structural information shared between the observed and missing samples. For example, the observed and missing data may share a common latent low-rank representation, as assumed in Non-negative Matrix Factorization, or they may lie in a union of multiple subspaces, as in subspace learning approaches. In this work, we focus on learning a smooth self-representation that effectively encodes this shared structure for each view, under the assumption that both the observed and missing data reside in a union of multiple subspaces. Specifically, for the v-th view, the observed data, missing data, and smooth self-representation are modeled as:

$$\left[\mathbf{X}_{\mathbf{o}}^{(v)}, \mathbf{X}_{\mathbf{m}}^{(v)}\right] = \left[\mathbf{X}_{\mathbf{o}}^{(v)}, \mathbf{X}_{\mathbf{m}}^{(v)}\right] \mathbf{Z}^{(v)} \tag{5}$$

where $\mathbf{Z}^{(v)}$ is the self-representation coefficient matrix for the v-th view, encoding the shared latent structure between observed and missing data. This matrix can thus be regarded as a smooth representation of the view. However, both $\mathbf{Z}^{(v)}$ and $\mathbf{X}_{\mathbf{m}}^{(v)}$ are unknown a priori, posing a central challenge for optimization. As shown in Eq. (4), we jointly learn $\mathbf{Z}^{(v)}$ in conjunction with structural graph learning. Accordingly, the representation learning term $\Phi\left(\mathbf{Z}^{(v)}, \left[\mathbf{X}_{\mathbf{o}}^{(v)}, \mathbf{X}_{\mathbf{m}}^{(v)}\right]\right)$ can be formulated as a subspace learning problem (Eq. (4)). Integrating this into our framework, the final optimization problem in Eq. (3) can be explicitly expressed as:

$$\begin{aligned}
&\min_{\mathbf{G}^{(v)},\mathbf{Z}^{(v)},\mathbf{X}_{\mathbf{m}}^{(v)}} \sum_{v=1}^{V}\sum_{v=1}^{V} \left\|\mathbf{Z}_i^{(v)} - \mathbf{Z}_j^{(v)}\right\|_2^2 \mathbf{S}_{i,j}^{(v)} + \alpha \left\|\mathbf{S}^{(v)}\right\|_F^2 \\
&+ \gamma \left\|\mathcal{S}\right\|_{\circledast} + \left\|\mathbf{Z}^{(v)}\right\|_F \\
&s.t.\ \ \mathbf{S}_i^{(v)\top}\mathbf{1} = 1; \mathbf{S}^{(v)} \succeq 0, \\
&\quad \left[\mathbf{X}_{\mathbf{o}}^{(v)}, \mathbf{X}_{\mathbf{m}}^{(v)}\right] = \left[\mathbf{X}_{\mathbf{o}}^{(v)}, \mathbf{X}_{\mathbf{m}}^{(v)}\right] \mathbf{Z}^{(v)}.
\end{aligned} \tag{6}$$

Overall, this unified formulation enables the simultaneous recovery of $\mathbf{X}_{\mathbf{m}}^{(v)}$, representation learning of $\mathbf{Z}^{(v)}$, adaptive graph learning, and view-consistency high-order structural modeling (via tensor learning) across multiple incomplete views.

3.2 MODEL OPTIMIZATION

In this section, we present the complete optimization procedure for the proposed model in detail.Given that the model involves multiple variables, the optimization problem is solved using an augmented Lagrangian multiplier (ALM) framework combined with an alternating direction minimization (ADM) strategy, in which variables are updated iteratively while keeping the others fixed.

Solve $\mathcal{S}$: To ensure the separability of $\mathcal{S}$, we employ a variable-splitting technique by introducing an auxiliary tensor $\mathcal{P} \in \mathbb{R}^{n\times n\times V}$ as a surrogate for $\mathcal{S}$. Accordingly, the model defined in Eq. equation 6 can be reformulated as the following constrained optimization problem:

$$\begin{aligned} &\min_{\mathbf{S}^{(v)}} \sum_{v=1}^{V} \left\| \mathbf{Z}_i^{(v)} - \mathbf{Z}_j^{(v)} \right\|_2^2 \mathbf{S}_{i,j}^{(v)} + \alpha \left\| \mathbf{S}^{(v)} \right\|_F^2 + \gamma \left\| \mathcal{P} \right\|_{\circledast} \\ &s.t.\ \ {\mathbf{S}_i^{(v)}}^{\top} \mathbf{1} = 1, \mathbf{S}^{(v)} \succeq 0, \mathcal{S} = \mathcal{P} \end{aligned} \tag{7}$$

The augmented Lagrangian function for the proposed model is formulated as follows:

$$\begin{aligned} &\min_{\mathbf{S}^{(v)}} \sum_{v=1}^{V} \left\| \mathbf{Z}_i^{(v)} - \mathbf{Z}_j^{(v)} \right\|_2^2 \mathbf{S}_{i,j}^{(v)} + \alpha \left\| \mathbf{S}^{(v)} \right\|_F^2 + \gamma \left\| \mathcal{P} \right\|_{\circledast} \\ &+ \frac{\rho}{2} \|\mathcal{P} - (\mathcal{S} + \frac{\mathcal{Q}}{\rho})\|_F^2 \\ &s.t.\ \ {\mathbf{S}_i^{(v)}}^{\top} \mathbf{1} = 1, \mathbf{S}^{(v)} \succeq 0, \mathcal{S} = \mathcal{P} \end{aligned} \tag{8}$$

where $\mathcal{Q} \in \mathbb{R}^{n\times n\times V}$ denotes the Lagrangian multipliers and $\rho > 0$ represents the penalty factor. Problem in Eq.equation 8 enables decomposition into several distinct subproblems via an alternating minimization strategy, with each variable optimized iteratively while maintaining others fixed.

$\mathbf{S}^{(v)}$-subproblem By fixing the other variables, the variable $\mathbf{S}^{(v)}$ is updated by solving the following problem:

$$\begin{aligned} &\min_{{\mathbf{S}_i^{(v)}}^{\top} \mathbf{1}=1,\, \mathbf{S}^{(v)}\succeq 0} \sum_{v=1}^{V} \sum_{i,j=1}^{n} \left\| \mathbf{z}_i^{(v)} - \mathbf{z}_j^{(v)} \right\|_2^2 s_{ij}^{(v)} + \alpha \left\| \mathbf{S}^{(v)} \right\|_F^2 \\ &+ \frac{\rho}{2} \left\| \mathbf{P}^{(v)} - \left(\mathbf{S}^{(v)} + \frac{\mathbf{Q}^{(v)}}{\rho} \right) \right\|_F^2 \end{aligned} \tag{9}$$

Denote $\mathbf{B}^{(v)} = \mathbf{P}^{(v)} - \frac{\mathbf{Q}^{(v)}}{\rho}$, for each view, equation equation 9 is transformed into the constrained minimization objective:

$$\begin{aligned} &\min_{{\mathbf{S}_i^{(v)}}^{\top} \mathbf{1}=1,\, \mathbf{S}^{(v)}\succeq 0} \sum_{i,j=1}^{n} \left\| z_i^{(v)} - z_j^{(v)} \right\|_2^2 s_{ij}^{(v)} + \alpha \left(s_{ij}^{(v)} \right)^2 \\ &+ \frac{\rho}{2} \left(b_{ij}^{(v)} - s_{ij}^{(v)} \right)^2. \end{aligned} \tag{10}$$

Let the distance vector $\mathbf{e}_i^{(v)}$ be defined with elements $e_{ij}^{(v)} = \left| z_i^{(v)} - z_j^{(v)} \right|_2^2$. With this definition, the problem in Eq. equation 10 can be reformulated for each sample i as follows:

$$\begin{aligned} &\min_{{\mathbf{S}_i^{(v)}}^{\top} \mathbf{1}=1,\, \mathbf{S}^{(v)}\succeq 0} \mathbf{e}_i^{(v)} \mathbf{s}_i^{(v)} + \alpha \left(\mathbf{s}_i^{(v)} \right)^2 \\ &+ \frac{\rho}{2} \left(\left(\mathbf{b}_i^{(v)} \right)^2 - 2\mathbf{b}_i^{(v)} \mathbf{s}_i^{(v)} + \left(\mathbf{s}_i^{(v)} \right)^2 \right) \end{aligned} \tag{11}$$

By algebraic manipulation, the problem can be reformulated as an equivalent simplex projection task. Thus, the above optimization is equivalent to solving the following model:

$$\min_{\mathbf{s}_i^{(v)\top}\mathbf{1}=1\ \mathbf{S}^{(v)}\succeq 0} \left\| \mathbf{s}_i^{(v)} - \frac{\rho \mathbf{b}_i^{(v)} - \mathbf{e}_i^{(v)}}{2\alpha + \rho} \right\|_2^2. \tag{12}$$

Specifically, the problem in Eq. equation 12 corresponds to a Euclidean projection onto the simplex, whose Lagrangian function, with dual variables η and φ, can be expressed as:

$$\begin{aligned} \mathcal{L}\left(\mathbf{s}_i^{(v)}, \eta, \varphi\right) &= \frac{1}{2} \left\| \mathbf{s}_i^{(v)} - \frac{\rho \mathbf{b}_i^{(v)} - \mathbf{e}_i^{(v)}}{2\alpha + \rho} \right\|_2^2 \\ &-\eta \left(\left(\mathbf{s}_i^{(v)}\right)^T \mathbf{1} - 1 \right) - \varphi^T \mathbf{s}_i^{(v)} \end{aligned} \tag{13}$$

where η is a scalar Lagrange multiplier and φ is a vector of Lagrange multipliers. The optimal solution under KKT conditions is given by:

$$\mathbf{s}_i^{(v)^*} = \left(\frac{\rho \mathbf{b}_i^{(v)} - \mathbf{e}_i^{(v)}}{2\alpha + \rho} + \eta \mathbf{1} \right)_+. \tag{14}$$

$\mathcal{P}$-subproblem By keeping all other variables fixed, the auxiliary tensor $\mathcal{P}$ is updated by solving the following subproblem:

$$\min_{\mathcal{P}} \gamma \|\mathcal{P}\|_{\circledast} + \frac{\rho}{2} \left\| \mathcal{P} - \left(\mathcal{S} + \frac{\mathcal{Q}}{\rho} \right) \right\|_F^2 \tag{15}$$

Denote $\mathcal{G} = \mathcal{S} + \frac{\mathcal{Q}}{\rho}$, the optimal solution can be computed by the tensor tubal-shrinkage operator (Hu et al. 2016):

$$\boldsymbol{P}^* = \boldsymbol{C}_{n_3\tau}(\boldsymbol{G}) = \boldsymbol{U} \otimes \boldsymbol{C}_{n_3\tau}(\boldsymbol{O}) \otimes \boldsymbol{V}^{\mathrm{T}}, \tag{16}$$

where $\tau = \gamma/\rho$, and $\boldsymbol{G} = \boldsymbol{U} \otimes \boldsymbol{O} \otimes \boldsymbol{V}^{\mathrm{T}}$ denotes the tensor SVD decomposition, and $\boldsymbol{C}_{n_3\tau}(\boldsymbol{O}) = \boldsymbol{O} \otimes \boldsymbol{J}$, herein, $\boldsymbol{J}$ is an $n_1 \times n_2 \times n_3$ f-diagonal tensor whose diagonal element in the Fourier domain is: $\boldsymbol{J}_f(i,i,j) = \left(1 - \frac{n_3\tau}{\boldsymbol{O}_f^{(j)}(i,i)}\right)_+$.

$\mathcal{Q}$ and ρ-subproblem The Lagrange multiplier $\mathcal{Q}$ and penalty factor ρ are iteratively updated according to:

$$\begin{aligned} \mathcal{Q} &= \mathcal{Q} + \rho(\mathcal{S} - \mathcal{P}) \\ \rho &= \mu * \rho \end{aligned} \tag{17}$$

where $\mu > 1$ accelerates convergence.

Solve $\mathbf{X}_{\mathbf{m}}^{(v)}$ Based on the learned representation $\mathbf{Z}^{(v)}$, the missing data $\mathbf{X}_{\mathbf{m}}^{(v)}$ can be estimated by solving the following subproblem:

$$\min_{\mathbf{X}_{\mathbf{m}}^{(v)}} \sum_{v=1}^{V} \left\| \left[\mathbf{X}_{\mathbf{o}}^{(v)}, \mathbf{X}_{\mathbf{m}}^{(v)} \right] - \left[\mathbf{X}_{\mathbf{o}}^{(v)}, \mathbf{X}_{\mathbf{m}}^{(v)} \right] \mathbf{Z}^{(v)} \right\|_F^2 \tag{18}$$

Both the observed and missing data share a common representation $\mathbf{Z}^v$, which facilitates the imputation of missing entries. This imputation strategy leads to the following optimization objective:

$$\min_{\mathbf{X}_{\mathbf{m}}^{(v)}} \operatorname{Tr}\left(\left[\mathbf{X}_{\mathbf{o}}^{(v)}, \mathbf{X}_{\mathbf{m}}^{(v)} \right] \mathbf{B}^{(v)} \left[\mathbf{X}_{\mathbf{o}}^{(v)}, \mathbf{X}_{\mathbf{m}}^{(v)} \right]^\top \right) \tag{19}$$

where $\mathbf{B}^{(v)} = \mathbf{I}_n - \mathbf{Z}^{(v)} - \mathbf{Z}^{(v)\top} + \mathbf{Z}^{(v)}\mathbf{Z}^{(v)\top}$, substitution of the block matrix form yields:

$$\min_{\mathbf{X}_{\mathbf{m}}^{(v)}} \operatorname{Tr}\left(\left[\mathbf{X}_{\mathbf{o}}^{(v)}, \mathbf{X}_{\mathbf{m}}^{(v)} \right] \begin{bmatrix} \mathbf{B}_{(oo)}^{(v)} & \mathbf{B}_{(om)}^{(v)} \\ \mathbf{B}_{(mo)}^{(v)} & \mathbf{B}_{(mm)}^{(v)} \end{bmatrix} \left[\mathbf{X}_{\mathbf{o}}^{(v)}, \mathbf{X}_{\mathbf{m}}^{(v)} \right]^\top \right) \tag{20}$$

Accordingly, Eq. equation 19 can be algebraically expanded as follows:

$$\min_{\mathbf{X}_{\mathbf{m}}^{(v)}} \operatorname{Tr}\left(\mathbf{X}_{\mathbf{m}}^{(v)}\mathbf{B}_{(mm)}^{(v)}\mathbf{X}_{\mathbf{m}}^{(v)\top} + \mathbf{X}_{\mathbf{o}}^{(v)}\left(\mathbf{B}_{(mo)}^{(v)\top} + \mathbf{B}_{(om)}^{(v)}\right)\mathbf{X}_{\mathbf{m}}^{(v)\top}\right) \tag{21}$$

From the definition of $\mathbf{B}^{(v)}$, we have

$$\mathbf{B}_{(mm)}^{(v)} = \left(\mathbf{I}_n - \mathbf{Z}^{(v)}\right)_{\mathbf{m}}^{\top}\left(\mathbf{I}_n - \mathbf{Z}^{(v)}\right)_{\mathbf{m}} \tag{22}$$

where $\left(\mathbf{I}_n - \mathbf{Z}^{(v)}\right)\mathbf{m}$ denotes the columns corresponding to the missing entries in the v-th view. The positive-definite nature of $\mathbf{B}_{(mm)}^{(v)}$ ensures that the optimal solution can be obtained by setting the derivative of the objective to zero, yielding:

$$\mathbf{X}_{\mathbf{m}}^{(v)} = -\mathbf{X}_{\mathbf{o}}^{(v)}\mathbf{B}_{(om)}^{(v)}\mathbf{B}_{(mm)}^{(v)-1} \tag{23}$$

Solve $\mathbf{Z}^{(v)}$ The smooth representation $\mathbf{Z}^{(v)}$ can be interpreted as a form of regularized subspace learning, where the objective is to reconstruct the original data while enforcing both regularization and structural consistency. The corresponding optimization problem can be formulated as:

$$\begin{aligned}\min_{\mathbf{Z}^{(v)}} &\sum_{v=1}^{V}\left\|\mathbf{X}^{(v)} - \mathbf{X}^{(v)}\mathbf{Z}^{(v)}\right\|_F^2 \\ &+ \lambda\sum_{v=1}^{V}\left\|\mathbf{Z}_i^{(v)} - \mathbf{Z}_j^{(v)}\right\|_2^2\mathbf{S}_{i,j}^{(v)}\end{aligned} \tag{24}$$

where $\mathbf{X}^{(v)} = \left[\mathbf{X}_{\mathbf{o}}^{(v)}, \mathbf{X}_{\mathbf{m}}^{(v)}\right]$. The objective can be transformed into

$$\min_{\mathbf{Z}^{(v)}}\sum_{v=1}^{V}\left\|\mathbf{X}^{(v)} - \mathbf{X}^{(v)}\mathbf{Z}^{(v)}\right\|_F + \lambda\operatorname{Tr}\left(\mathbf{Z}^{(v)}\mathbf{L}_s^{(v)}\mathbf{Z}^{(v)\top}\right) \tag{25}$$

Let $\mathbf{L}_s^{(v)}$ denote the Laplacian matrix corresponding to $\mathbf{S}$. By setting the partial derivative of the objective function with respect to $\mathbf{Z}^{(v)}$ to zero, the closed-form solution can be obtained as:

$$\mathbf{X}^{(v)\top}\mathbf{X}^{(v)}\mathbf{Z}^{(v)} - \mathbf{X}^{(v)\top}\mathbf{X}^{(v)} + \lambda\mathbf{L}_s^{(v)}\mathbf{Z}^{(v)} = 0 \tag{26}$$

Consequently, the closed-form solution can be expressed as:

$$\mathbf{Z}^{(v)} = \left(\mathbf{X}^{(v)\top}\mathbf{X}^{(v)} + \lambda\mathbf{L}_s^{(v)}\right)^{-1}\mathbf{X}^{(v)\top}\mathbf{X}^{(v)}. \tag{27}$$

4 Experiment

4.1 Experiment Settings

4.1.1 **Datasets.**

We evaluate our method and competing approaches on eight multi-view datasets: BBCSport Greene & Cunningham (2006), Yale Belhumeur et al. (1996), ORL Samaria & Harter (1994), Olympics Greene & Cunningham (2013), Still Delaitre et al. (2010), BBC Greene & Cunningham (2006), Buaa Wang et al. (2010), and Leaves Beghin et al. (2010). Following common IMVC settings, we randomly remove views with missing ratios $r \in \{0.1, 0.3, 0.5\}$, while ensuring that each sample has at least one observed view.

4.1.2 **Compared Methods.**

We compare the proposed method against the following state-of-the-art incomplete multi-view clustering approaches: UEAF Wen et al. (2019), GIMC-FLSD Wen et al. (2021), IMSR Liu et al. (2021a), HCLS-CGL Wen et al. (2023b), SEMI Wang et al. (2024), LaSA Liu et al. (2024a), and BWIC-TIMC Yao et al. (2025).

Table 1: Clustering performance on eight datasets under different missing ratios.

Dataset	Method	ACC			NMI			Purity		
		0.1	0.3	0.5	0.1	0.3	0.5	0.1	0.3	0.5
ORL	UEAF	0.5620	0.4950	0.3300	0.7293	0.6399	0.4728	0.6148	0.5400	0.3725
	GIMC-FLSD	0.6550	0.5625	0.4600	0.7884	0.7057	0.6374	0.6875	0.5725	0.4800
	HCLS-CGL	0.6775	0.6163	0.5100	0.8006	0.7627	0.6898	0.7025	0.6553	0.5400
	IMSR	0.6750	0.5653	0.4673	0.8113	0.7225	0.6577	0.7075	0.5895	0.5045
	SEMI	0.7885	0.7098	0.5102	0.8905	0.8555	0.7021	0.8172	0.7527	0.5573
	LaSA	0.8262	0.7713	0.6175	0.8963	0.8559	0.7563	0.8368	0.7853	0.6333
	BWIC-TIMC	0.7480	0.7065	0.5735	0.8623	0.8238	0.7284	0.7611	0.7395	0.6075
	Ours	**0.8548**	**0.7955**	**0.6705**	**0.9022**	**0.8775**	**0.7877**	**0.8725**	**0.8145**	**0.6915**
BBC	UEAF	0.7547	0.7241	0.6175	0.5784	0.5438	0.4095	0.7547	0.7241	0.6642
	GIMC-FLSD	0.7591	0.7696	0.7632	0.5739	0.5755	0.5524	0.7591	0.7696	0.7641
	HCLS-CGL	0.8861	0.8263	0.7956	0.6938	0.6198	0.5806	0.8861	0.8263	0.7956
	IMSR	0.9003	0.8550	0.7934	0.7407	0.6747	0.5647	0.9003	0.8550	0.8035
	SEMI	0.8859	0.8778	0.8482	0.7315	0.7177	0.6545	0.8859	0.8778	0.8482
	LaSA	0.8613	0.7956	0.7796	0.6875	0.6466	0.6196	0.8613	0.8029	0.8058
	BWIC-TIMC	0.8782	0.8365	0.8184	0.7059	0.6338	0.6005	0.8782	0.8365	0.8184
	Ours	**0.9469**	**0.9107**	**0.8585**	**0.8442**	**0.7691**	**0.6910**	**0.9469**	**0.9107**	**0.8585**
BBCSport	UEFA	0.7822	0.7724	0.6931	0.7071	0.6825	0.5513	0.8741	0.8707	0.7707
	GIMC_FLSD	0.7759	0.7414	0.6466	0.6581	0.6002	0.4455	0.8793	0.8362	0.7155
	HCLS_CGL	0.8103	0.7845	0.7414	0.6886	0.6459	0.5765	0.8707	0.8621	0.8190
	IMSR	0.7966	0.7362	0.6543	0.7399	0.6586	0.4984	0.8940	0.8466	0.7431
	SEMI	0.7952	0.7871	0.7616	0.7255	0.7104	0.6716	0.8959	0.8821	0.8528
	LaSA	**0.8655**	0.8129	0.6750	0.7847	0.6943	0.5381	0.8931	0.8517	0.7431
	BWIC-TIMC	0.7914	0.7471	0.6628	0.7376	0.6634	0.5490	0.8662	0.8160	0.7531
	Ours	0.8474	**0.8138**	**0.7841**	**0.8358**	**0.7334**	**0.6733**	**0.9422**	**0.8943**	**0.8581**
Yale	UEFA	0.6061	0.5030	0.3091	0.6717	0.5085	0.3348	0.6061	0.5152	0.3273
	GIMC_FLSD	0.6303	0.5879	0.4061	0.6387	0.6133	0.4446	0.6303	0.5879	0.4242
	HCLS_CGL	0.6606	0.6303	0.4909	0.6710	0.6747	0.5391	0.6667	0.6364	0.4909
	IMSR	0.6527	0.6412	0.5442	0.6741	0.6553	0.5680	0.6533	0.6436	0.5545
	SEMI	0.6520	0.6335	0.5893	0.6808	0.6573	0.6183	0.6577	0.6401	0.5977
	LaSA	0.7012	0.6715	0.5442	0.7258	0.6967	0.5805	0.7012	0.6745	0.5485
	BWIC-TIMC	0.6830	0.6612	0.5325	0.6985	0.6709	0.5649	0.6833	0.6653	0.5457
	Ours	**0.7552**	**0.7115**	**0.6012**	**0.7882**	**0.7432**	**0.6342**	**0.7552**	**0.7127**	**0.6048**
Leaves	UEFA	0.6719	0.4063	0.2794	0.8121	0.6442	0.5291	0.6938	0.4294	0.3013
	GIMC_FLSD	0.5294	0.3613	0.3419	0.7465	0.6261	0.6159	0.5631	0.3881	0.3681
	HCLS_CGL	0.6256	0.6088	0.4575	0.7876	0.7743	0.7093	0.6500	0.6325	0.4831
	IMSR	0.6612	0.4866	0.3391	0.8159	0.7192	0.6271	0.6828	0.5101	0.3604
	SEMI	0.7118	0.5542	0.4442	0.8499	0.7494	0.6809	0.7382	0.5801	0.4696
	LaSA	0.8756	0.7628	0.5269	0.9172	0.8509	0.7364	0.8831	0.7703	0.5463
	BWIC-TIMC	0.8196	0.7528	0.5041	0.8931	0.8491	0.7323	0.8323	0.7690	0.5335
	Ours	**0.9091**	**0.7867**	**0.5399**	**0.9471**	**0.8889**	**0.7494**	**0.9167**	**0.7993**	**0.5661**
Buaa	UEFA	0.3304	0.2785	0.2570	0.6440	0.5707	0.6066	0.3563	0.3007	0.2748
	GIMC_FLSD	0.3430	0.2926	0.2696	0.6610	0.6353	0.6297	0.3570	0.3074	0.2837
	HCLS_CGL	0.4704	0.4126	0.3267	0.7345	0.7029	0.6662	0.4815	0.4237	0.3481
	IMSR	0.5635	0.4694	0.3580	0.7851	0.7350	0.6849	0.5844	0.4924	0.3844
	SEMI	0.4891	0.4061	0.3588	0.7424	0.6992	0.6800	0.5117	0.4306	0.3845
	LaSA	0.5237	0.4711	0.3242	0.7615	0.7318	0.6692	0.5363	0.4881	0.3472
	BWIC-TIMC	0.5127	0.4652	0.3382	0.7553	0.7328	0.6742	0.5321	0.4856	0.3640
	Ours	**0.6861**	**0.5719**	**0.3641**	**0.8485**	**0.7847**	**0.6917**	**0.7014**	**0.5870**	**0.3941**
Olympics	UEFA	0.6056	0.5496	0.3879	0.7086	0.6676	0.5561	0.7004	0.6509	0.5453
	GIMC_FLSD	0.6789	0.6250	0.4095	0.7801	0.6999	0.6037	0.7672	0.6832	0.5819
	HCLS_CGL	0.6595	0.6487	0.4547	0.7813	0.7663	0.6661	0.8039	0.7651	0.6530
	IMSR	0.7397	0.7101	0.4616	0.8024	0.7920	0.6843	0.8002	0.7959	0.6526
	SEMI	0.7349	0.6936	0.6500	0.8140	0.7823	0.7533	0.8100	0.7775	0.7513
	LaSA	0.6879	0.6769	0.4599	0.8167	0.7959	0.6749	0.8088	0.7886	0.6534
	BWIC-TIMC	0.7103	0.6895	0.4474	0.8171	0.7990	0.6579	0.8336	0.8081	0.6241
	Ours	**0.7922**	**0.7761**	**0.6981**	**0.8414**	**0.8344**	**0.7862**	**0.8607**	**0.8528**	**0.7957**
Still	UEFA	0.2869	0.2805	0.2827	0.0791	0.0980	0.0715	0.3148	0.3340	0.3062
	GIMC_FLSD	0.3105	0.2869	0.2955	0.1035	0.0917	0.0718	0.3255	0.3169	0.3041
	HCLS_CGL	0.3126	0.2964	0.3041	0.1033	0.0997	0.0903	0.3340	0.3227	0.3340
	IMSR	0.3073	0.3073	0.2737	0.1174	0.1021	0.0664	0.3390	0.3355	0.3054
	SEMI	0.2904	0.2860	0.2862	0.1157	0.0975	0.0952	0.3250	0.3184	0.3174
	LaSA	0.2966	0.2837	0.2630	0.0872	0.0879	0.0701	0.3197	0.3197	0.2884
	BWIC-TIMC	0.3161	0.2931	0.2832	0.0955	0.0829	0.0764	0.3460	0.3185	0.3061
	Ours	**0.4161**	**0.4049**	**0.3180**	**0.1988**	**0.1853**	**0.1189**	**0.4392**	**0.4315**	**0.3486**

Table 2: Ablation study results comparing Ours, Without S, and Fusion Z approaches

Dataset	Method	ACC			NMI			Purity		
		10%	30%	50%	10%	30%	50%	10%	30%	50%
Leaves	Ours	**0.9091**	**0.7867**	**0.5399**	**0.9471**	**0.8889**	**0.7494**	**0.9167**	**0.7993**	**0.5661**
	Variant-1	0.7943	0.5880	0.3977	0.8803	0.7610	0.6686	0.8086	0.6074	0.4282
	Variant-2	0.6477	0.4629	0.3257	0.8121	0.6942	0.6104	0.6721	0.4844	0.3462
BBC	Ours	**0.9469**	**0.9107**	**0.8585**	**0.8442**	**0.7691**	**0.6910**	**0.9469**	**0.9107**	**0.8585**
	Variant-1	0.7108	0.5016	0.5018	0.4877	0.3116	0.3214	0.7273	0.5564	0.5599
	Variant-2	0.8766	0.8492	0.5653	0.7289	0.6748	0.3929	0.8766	0.8492	0.6359
ORL	Ours	**0.8548**	**0.7955**	**0.6705**	**0.9022**	**0.8775**	**0.7877**	**0.8725**	**0.8145**	**0.6915**
	Variant-1	0.7082	0.5885	0.3492	0.8283	0.7377	0.5685	0.7428	0.6133	0.3705
	Variant-2	0.6545	0.5540	0.3732	0.7970	0.7104	0.5879	0.6903	0.5813	0.4037

4.1.3 EVALUATION METRICS

Clustering performance is evaluated using three widely adopted metrics: accuracy (ACC), normalized mutual information (NMI), and purity (PUR), where higher values indicate better clustering quality.

4.2 COMPARISON RESULTS

Tables 1 summarize the clustering performance of all compared IMVC methods on eight benchmark datasets under different missing ratios. The best result for each metric is highlighted in bold. Based on these results, we draw the following observations: The proposed method delivers the best overall performance across the eight datasets and three missing ratios. It consistently achieves superior ACC, NMI, and Purity compared with the seven state-of-the-art competitors, which verifies the effectiveness and robustness of the proposed unified optimization framework. Compared with representative imputation-based methods, including IMSR and LaSA, our method obtains consistently better results. This demonstrates that the proposed representation-induced view recovery mechanism can more reliably reconstruct missing views and exploit cross-view complementary information, leading to more discriminative representations for clustering.

4.3 ABLATION STUDY

To evaluate the effectiveness of key components, we conduct ablation studies with two variants: (1) Variant-1 removes the tensorized graph learning module; (2) Variant-2 removes smooth representation learning. The full model and its variants are evaluated on Leaves, BBC, and ORL under three missing ratios. The results are reported in Table 2.

As shown in Table 2, the full model consistently outperforms both variants across all metrics. Compared with Variant-1, it achieves average improvements of 23.69%, 21.02%, and 21.80% in ACC, NMI, and Purity, respectively. Compared with Variant-2, the corresponding gains are 21.82%, 16.09%, and 20.41%. These results verify that both tensorized graph learning and smooth representation learning are essential and complementary for robust incomplete multi-view clustering.

5 CONCLUSION

In this paper, we proposed a novel framework to unify latent tensorized graph learning with representation-induced view recovery for IMVC problem. By jointly optimizing tensorized graph structures and smooth, discriminative representations, our method effectively preserves cross-view consistency while accurately recovering missing information. Extensive experiments on eight real-world datasets under various missing ratios demonstrated that our approach consistently outperforms state-of-the-art IMVC methods.

AI USE STATEMENT

In this work, we used generative AI tools solely for language polishing and grammatical refinement to improve the clarity and readability of the manuscript. Generative AI tools were not used for generating research ideas, developing methodologies, conducting experiments, analyzing results, or drawing scientific conclusions. All AI-assisted text was carefully reviewed and revised by the authors to ensure its accuracy and consistency with the original scientific content. We take full responsibility for the final content of this work, including any text produced with the aid of generative AI.

REPRODUCIBILITY STATEMENT

To ensure the reproducibility of our work, we provide the source code in the supplementary materials. The main paper presents the proposed method and its implementation details, including the model architecture, training procedures, and experimental settings. The supplementary materials further provide the source code and additional experimental details to facilitate the reproduction of our results. We believe that these resources will enable researchers to reproduce our experiments and verify the effectiveness of the proposed method.

REFERENCES

Thibaut Beghin, James S Cope, Paolo Remagnino, and Sarah Barman. Shape and texture based plant leaf classification. In *International conference on advanced concepts for intelligent vision systems*, pp. 345–353. Springer, 2010.

Peter N Belhumeur, Joao P Hespanha, and David J Kriegman. Eigenfaces vs. fisherfaces: Recognition using class specific linear projection. In *European conference on computer vision*, pp. 43–58. Springer, 1996.

Yiran Cai, Hangjun Che, Baicheng Pan, Man-Fai Leung, Cheng Liu, and Shiping Wen. Projected cross-view learning for unbalanced incomplete multi-view clustering. *Information Fusion*, 105: 102245, 2024.

G. Chao, S. Wang, S. Yang, C. Li, and D. Chu. Incomplete multi-view clustering with multiple imputation and ensemble clustering. *Applied Intelligence*, 52(13):14811–14821, 2022.

Guoqing Chao, Shiliang Sun, and Jinbo Bi. A survey on multiview clustering. *IEEE Transactions on Artificial Intelligence*, 2(2):146–168, 2021.

Man-Sheng Chen, Ling Huang, Chang-Dong Wang, and Dong Huang. Multi-view clustering in latent embedding space. In *Proceedings of the AAAI Conference on Artificial Intelligence*, volume 34, pp. 3513–3520, 2020.

Jinrong Cui, Yulu Fu, Cheng Huang, and Jie Wen. Low-rank graph completion-based incomplete multiview clustering. *IEEE Transactions on Neural Networks and Learning Systems*, 35(6): 8064–8074, 2022.

Vincent Delaitre, Ivan Laptev, and Josef Sivic. Recognizing human actions in still images: a study of bag-of-features and part-based representations. In *British Machine Vision Conference (BMVC 2010)*, pp. 1–11, 2010.

Derek Greene and Padraig Cunningham. Practical solutions to the problem of diagonal dominance in kernel document clustering. In *Proceedings of International Conference on Machine Learning*, volume 148, pp. 377–384, 2006.

Derek Greene and Pádraig Cunningham. Producing a unified graph representation from multiple social network views. In *Proceedings of the 5th Annual ACM Web Science Conference*, pp. 118–121, 2013.

Jun Guo and Jiahui Ye. Anchors bring ease: An embarrassingly simple approach to partial multi-view clustering. In *Proceedings of the AAAI conference on artificial intelligence*, volume 33, pp. 118–125, 2019.

Menglei Hu and Songcan Chen. Doubly aligned incomplete multi-view clustering. In *Proceedings of the International Joint Conference on Artificial Intelligence*, pp. 2262–2268, 2018.

Menglei Hu and Songcan Chen. One-pass incomplete multi-view clustering. In *Proceedings of the AAAI Conference on Artificial Intelligence*, pp. 3838–3845, 2019.

Miaomiao Li, Siwei Wang, Xinwang Liu, and Suyuan Liu. Parameter-free and scalable incomplete multiview clustering with prototype graph. *IEEE Transactions on Neural Networks and Learning Systems*, 35(1):300–310, 2022.

S. Li, Y. Jiang, and Z.-H. Zhou. Partial multi-view clustering. In *Proceedings of the AAAI Conference on Artificial Intelligence*, pp. 1968–1974, 2014.

Zhaoyang Li, Qianqian Wang, Zhiqiang Tao, Quanxue Gao, and Zhaohua Yang. Deep adversarial multi-view clustering network. In *Proceedings of the International Joint Conference on Artificial Intelligence*, pp. 2952–2958, 2019.

Tianhai Liang, Qiangqiang Shen, Shuqin Wang, Yongyong Chen, Guokai Zhang, and Junxin Chen. Data completion-guided unified graph learning for incomplete multi-view clustering. *ACM Transactions on Knowledge Discovery from Data*, 18(8):188, 2024.

Yijie Lin, Yifei Gou, Zhaoyang Liu, Jinfeng Bai, Jiafeng Lv, and Xi Peng. COMPLETER: Incomplete multi-view clustering via contrastive prediction. In *Proceedings of the IEEE/CVF Conference on Computer Vision and Pattern Recognition*, pp. 11174–11183, 2021.

Cheng Liu, Rui Li, Si Wu, Hangjun Che, Dazhi Jiang, Zhiwen Yu, and Hau-San Wong. Self-guided partial graph propagation for incomplete multiview clustering. *IEEE Transactions on Neural Networks and Learning Systems*, 35(8):10803–10816, 2023a.

Cheng Liu, Si Wu, Rui Li, Dazhi Jiang, and Hau-San Wong. Self-supervised graph completion for incomplete multi-view clustering. *IEEE Transactions on Knowledge and Data Engineering*, 35(9): 9394–9406, 2023b.

Cheng Liu, Rui Li, Hangjun Che, Man-Fai Leung, Si Wu, Zhiwen Yu, and Hau-San Wong. Latent structure-aware view recovery for incomplete multi-view clustering. *IEEE Transactions on Knowledge and Data Engineering*, 36(12):8655–8669, 2024a.

Chengliang Liu, Zhaowen Wu, Jie Wen, Yong Xu, and Chao Huang. Localized sparse incomplete multi-view clustering. *IEEE Transactions on Multimedia*, 25:5539–5551, 2022.

Chengliang Liu, Jie Wen, Zhihao Wu, Xiaoling Luo, Chao Huang, and Yong Xu. Information recovery-driven deep incomplete multiview clustering network. *IEEE Transactions on Neural Networks and Learning Systems*, 35(11):15442–15452, 2024b.

Jiyuan Liu, Xinwang Liu, Yi Zhang, Pei Zhang, Wenxuan Tu, Siwei Wang, Sihang Zhou, Weixuan Liang, Siqi Wang, and Yuexiang Yang. Self-representation subspace clustering for incomplete multi-view data. In *Proceedings of the 29th ACM International Conference on Multimedia*, pp. 2726–2734, 2021a.

Xinwang Liu, Xinzhong Zhu, Miaomiao Li, Lei Wang, Chang Tang, Jianping Yin, Dinggang Shen, Huaimin Wang, and Wen Gao. Late fusion incomplete multi-view clustering. *IEEE transactions on pattern analysis and machine intelligence*, 41(10):2410–2423, 2018.

Xinwang Liu, Miaomiao Li, Chang Tang, Jingyuan Xia, Jian Xiong, Li Liu, Marius Kloft, and En Zhu. Efficient and effective regularized incomplete multi-view clustering. *IEEE Transactions on Pattern Analysis and Machine Intelligence*, 43(8):2634–2646, 2021b.

Zhenjiao Liu, Zhikui Chen, Yue Li, Liang Zhao, Tao Yang, Reza Farahbakhsh, Noel Crespi, and Xiaodi Huang. Imc-nlt: Incomplete multi-view clustering by nmf and low-rank tensor. *Expert Systems with Applications*, 221:119742, 2023c.

N. Rai, S. Negi, S. Chaudhury, and O. Deshmukh. Partial multi-view clustering using graph regularized nmf. In *Proceedings of the International Conference on Pattern Recognition*, pp. 2192–2197, 2016.

Ferdinando S Samaria and Andy C Harter. Parameterisation of a stochastic model for human face identification. In *Proceedings of 1994 IEEE workshop on applications of computer vision*, pp. 138–142, 1994.

Weixiang Shao, Lifang He, and Philip S. Yu. Multiple incomplete views clustering via weighted nonnegative matrix factorization with l2,1 regularization. In *Joint European Conference on Machine Learning and Knowledge Discovery in Databases*, pp. 318–334, 2015.

Huayi Tang and Yong Liu. Deep safe incomplete multi-view clustering: Theorem and algorithm. In *International conference on machine learning*, pp. 21090–21110. PMLR, 2022.

Qianqian Wang, Zhengming Ding, Zhiqiang Tao, Quanxue Gao, and Yun Fu. Partial multi-view clustering via consistent gan. In *2018 IEEE International Conference on Data Mining (ICDM)*, pp. 1290–1295, 2018.

Qianqian Wang, Zhengming Ding, Zhiqiang Tao, Quanxue Gao, and Yun Fu. Generative partial multi-view clustering with adaptive fusion and cycle consistency. *IEEE Transactions on Image Processing*, 30:1771–1783, 2021.

Xiaokan Wang, Xia Mao, and Catalin-Daniel Caleanu. Nonlinear shape-texture manifold learning. *IEICE Transactions on Information and Systems*, E93-D(7):2016–2019, 2010.

Yiming Wang, Dongxia Chang, Zhiqiang Fu, Jie Wen, and Yao Zhao. Incomplete multiview clustering via cross-view relation transfer. *IEEE Transactions on Circuits and Systems for Video Technology*, 33(1):367–378, 2022.

Ziyu Wang, Lusi Li, Xin Ning, Wenkai Tan, Yongxin Liu, and Houbing Song. Incomplete multi-view clustering via structure exploration and missing-view inference. *Information Fusion*, 103(000):12, 2024.

J. Wen et al. Deep double incomplete multi-view multi-label learning with incomplete labels and missing views. *IEEE Transactions on Neural Networks and Learning Systems*, 35(8):11396–11408, Aug. 2023a.

Jie Wen, Zheng Zhang, Yong Xu, Bob Zhang, Lunke Fei, and Hong Liu. Unified embedding alignment with missing views inferring for incomplete multi-view clustering. In *Proceedings of the AAAI conference on artificial intelligence*, volume 33, pp. 5393–5400, 2019.

Jie Wen, Yong Xu, and Hong Liu. Incomplete multiview spectral clustering with adaptive graph learning. *IEEE Transactions on Cybernetics*, 50(4):1418–1429, 2020.

Jie Wen, Zheng Zhang, Zhao Zhang, Lunke Fei, and Meng Wang. Generalized incomplete multiview clustering with flexible locality structure diffusion. *IEEE Transactions on Cybernetics*, 51(1): 101–114, 2021.

Jie Wen, Chengliang Liu, et al. Highly confident local structure based consensus graph learning for incomplete multi-view clustering. In *Proceedings of the IEEE/CVF Conference on Computer Vision and Pattern Recognition*, pp. 15712–15721, 2023b.

Jie Wen, Zheng Zhang, Zhao Zhang, Lunke Fei, and Bob Zhang. A survey on incomplete multiview clustering. *IEEE Transactions on Systems, Man, and Cybernetics: Systems*, 53(2):1136–1149, 2023c.

Cai Xu, Ziyu Guan, Wei Zhao, Hongchang Wu, Yunfei Niu, and Beilei Ling. Adversarial incomplete multi-view clustering. In *Proceedings of the Twenty-Eighth International Joint Conference on Artificial Intelligence*, pp. 3933–3939. International Joint Conferences on Artificial Intelligence Organization, 2019.

Jie Xu, Chao Li, Yazhou Ren, Liang Peng, Yujie Mo, Xiaoshuang Shi, and Xiaofeng Zhu. Deep incomplete multi-view clustering via mining cluster complementarity. In *Proceedings of the AAAI conference on artificial intelligence*, volume 36, pp. 8761–8769, 2022.

Mingze Yao, Huibing Wang, Yawei Chen, and Xianping Fu. Between/within view information completing for tensorial incomplete multi-view clustering. *IEEE Transactions on Multimedia*, 27: 1538–1550, 2025.

Changqing Zhang, Qinghua Hu, Huazhu Fu, Pengfei Zhu, and Xiaochun Cao. Latent multi-view subspace clustering. In *Proceedings of the IEEE Conference on Computer Vision and Pattern Recognition*, pp. 4279–4287, 2017.

Chao Zhang, Jingwen Wei, Bo Wang, Zechao Li, Chunlin Chen, and Huaxiong Li. Robust spectral embedding completion based incomplete multi-view clustering. In *Proceedings of the 31st ACM international conference on multimedia*, pp. 300–308, 2023.

Tao Zhang, Yunhao Yuan, Xiaobo Shen, and Fan Liu. Two-step affinity matrix learning for multi-view subspace clustering. *Expert Systems with Applications*, 242:122765, 2024.

Yi Zhang, Xinwang Liu, Siwei Wang, Jiyuan Liu, Sisi Dai, and En Zhu. One-stage incomplete multi-view clustering via late fusion. In *Proceedings of the 29th ACM international conference on multimedia*, pp. 2717–2725, 2021.

Wei Zhao, Cai Xu, Ziyu Guan, and Ying Liu. Multiview concept learning via deep matrix factorization. *IEEE Transactions on Neural Networks and Learning Systems*, 32(2):814–825, 2021.